

Flexible and Printed Electronics



TOPICAL REVIEW

Flexible perovskite solar cells: device design and perspective

RECEIVED
11 September 2019

REVISED
10 October 2019

ACCEPTED FOR PUBLICATION
7 November 2019

PUBLISHED
12 February 2020

Juan Long^{1,2}, Zengqi Huang^{1,2}, Jiaqi Zhang^{1,2}, Xiaotian Hu^{1,4,2} , Licheng Tan^{1,2,4}  and Yiwang Chen^{1,2,3,4} 

¹ College of Chemistry, Nanchang University, 999 Xuefu Avenue, Nanchang 330031, People's Republic of China

² Institute of Polymers and Energy Chemistry, Nanchang University, 999 Xuefu Avenue, Nanchang 330031, People's Republic of China

³ Institute of Advanced Scientific Research (IASR), Jiangxi Normal University, 99 Ziyang Avenue, Nanchang 330022, People's Republic of China

⁴ Authors to whom any correspondence should be addressed.

E-mail: xiaotian@iccas.ac.cn, tanlicheng@ncu.edu.cn and ywchen@ncu.edu.cn

Keywords: perovskite solar cells, flexible devices, large-area processes

Abstract

Flexible perovskite solar cells (FPSCs) have gained more and more attention in a short period of time, attributing to their unique properties, which including being lightweight, and its flexibility, compatibility and stretchability with curved surfaces. So far, the FPSCs have obtained notable milestones and the champion-cell efficiency has achieved 19.11%. In the meanwhile, the advantage of extraordinary ease of processing for large-area flexible devices, permits their employ in niche applications, such as vehicle-integrated photovoltaics, portable electronics, wearable power sources, and large-scale industrial roofing, etc. In this review paper, we retrospect recent developments in FPSCs, focusing on the device design and materials selection of the substrate, the transparent electrodes and the interface layers. Moreover, we summarize the large-area processes for fabricating scalable flexible devices. In addition, some promising research directions are provided for the future design of FPSCs.

1. Introduction

In the development of photovoltaic cells, a wide variety of solar cells, i.e.: crystalline silicon [1–6], thin film PV (e.g. CdTe [7, 8], CIGS [9, 10], CZTS [11–13], GaAs [14]), dye-sensitized solar cells (DSSCs) [15], quantum dot-sensitized solar cells [16], organic solar cells [17], and perovskite solar cells (PSCs) [18], have received extensive research attentions. However, there has been no solar cell like the PSCs and the power conversion efficiencies (PCEs) have improved rapidly in a short period of time, from the first reported PCE of 3.81% [19] to a record value of 25.2% [20]. The reasons why perovskites can get so much attention are attributed to their novel material characteristics, which include a high optical absorption coefficient, long-range charge carrier diffusion lengths, low exciton binding energies, and the easy tuning of the band gaps via simple interchanges of the precursor components [21].

But beyond that, existing PSCs have been unable to meet practical demand, and portable, wearable products have become a hot research direction. Therefore, flexible perovskite solar cells (FPSCs) have gained more and more attention on account of their

advantageous characteristics, including being lightweight, and their flexibility, compatibility and stretchability with curved surfaces [2]. Based on this, it has great application value in various fields, for example, vehicle-integrated photovoltaics, building-integrated photovoltaics, wearable power sources and so on [22]. The wide application of FPSCs in these fields will greatly improve the quality of human life.

In recent years, scientists have overcome many difficulties, solved many problems during the FPSC research process, and relevant conclusions have been published in papers. In 2013, Kumar and co-workers used a low-temperature method to prepare zinc oxide (ZnO) nanorods as an electron transport layer (ETL). It is the first time to get a flexible device with a PCE of 2.62% [23]. In the following years, with the development of new transparent electrode materials and perovskite films suitable for FPSCs, the performance of FPSCs has been greatly improved. In 2014, Jung and co-workers inserted an additional buffer layer to heighten the ohmic contact between the metal electrode and PCBM layer, and prepared a PCE of 9.4% inverted structure FPSCs [24]. In 2015, Shin and co-workers prepared a Zn₂SO₄ nanocrystalline film with a

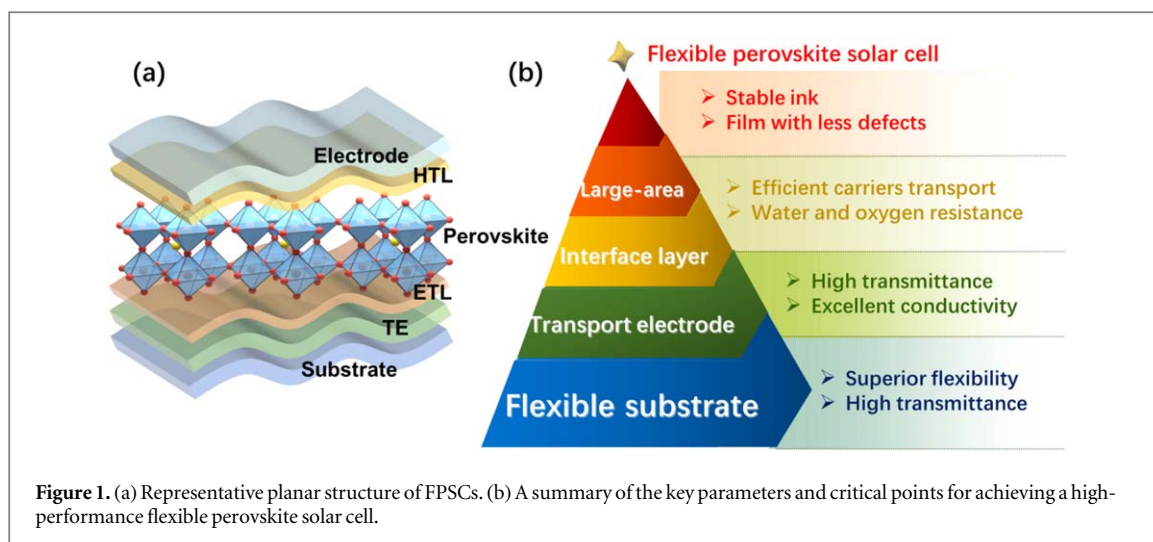


Figure 1. (a) Representative planar structure of FPSCs. (b) A summary of the key parameters and critical points for achieving a high-performance flexible perovskite solar cell.

better optical transmittance to replace the traditional titanium oxide (TiO_2) for ETL in FPSCs. And the PCE of the optimized devices enhanced to 15.3% [25]. Subsequently, in 2016, they developed a spin-coated Zn_2SO_4 nano-ink as an ETL. The efficiency further improved to 16.5% [26]. In 2017, Yoon and co-workers prepared a FPSC with a PCE of 17.3% on indium tin oxide (ITO) transparent electrodes [27]. In the same year, Huang and co-workers fabricated FPSC on an ITO/polyethylene terephthalate (PET) substrate using the low-temperature solution method, and the device obtained an efficiency of 18.1% [28]. Recently, Cao and co-workers fabricated a FPSC based on polyethylene naphthalate (PEN) /ITO substrates, which achieved a record PCE of 19.11% [29]. Undoubtedly, through the efforts of many scientists, the performance of FPSCs will be greatly improved in the near future.

However, the poor long-term stability and relatively low PCE are important factors limiting the development of FPSCs. Compared to rigid PSC fabricated on a glass substrate, each layer that makes up the complete FPSC device has some special requirement, including the substrate, the transparent electrodes (TE), ETL, the perovskite layer, the hole transport layer (HTL) and the electrode, as shown in figure 1(a). The low-temperature preparation demand becomes a stumbling block to achieve high efficiency. In addition, stretchability and robust bending durability are also important indicators for achieving the long-term stability. Another challenge that we ought to face is the large-scale manufacturing process, and the further commercial development will be limited due to this difficulty. Even though, there is still plenty of space to surpass rigid PSCs in the future, especially showing promising commercial potential in the development of large-area modules.

In this review, we examine the recent advance on FPSCs from the different views of functional layers, which includes a flexible substrate, transparent electrode, and interface layer, as shown in figure 1(b).

Furthermore, we summarize the important advance of large-area FPSCs in recent years. Finally, the promising perspectives on the development of FPSCs will be taken out.

2. Substrate choices for FPSCs

The substrate is essential to the high-performance FPSCs, superior flexibility and high transmittance are the major elements of the substrate. These categories of materials, i.e., polymers, metal foils, ultrathin flexible glass, muscovite mica and nanopaper, are available for the substrate of FPSCs. The benefits and drawbacks of these substrates are discussed as follows. In addition to excellent flexibility and transmittance, polymer substrates also possess the benefits of being lightweight, low cost, and having roll-to-roll processability, etc. PET and PEN are commonly employed as flexible substrates. However, low glass transition temperature (T_g), a high coefficient of thermal expansion (CTE) of $\sim 20/^\circ\text{C}$ and poor gas barrier performance limited its application in FPSCs [30]. In particular, the shrinkage of the PET substrate would occur during high temperature treatment (figure 2(a)) [31]. Therefore, the temperature in the whole fabrication process is critical to obtain a high-performance FPSC. The fabricating temperature of PET and PEN should be below 150°C , whereas colorless polyimide (CPI) can be fabricated above 150°C on account of the higher T_g (figure 2(b)) [32, 33]. Park and co-workers processed high-performance FPSCs based on CPI/ITO substrate, and the device yield a PCE of 15.5%. The substrates undergo a high temperature of 300°C during the whole fabrication process [34]. They successfully find an useful way to overcome the temperature limitation.

In contrast to polymer substrates, metal substrates offer special superiorities, such as distinguished thermal stability, high barrier properties, and ultra-low sheet resistance [39]. However, due to the opacity of

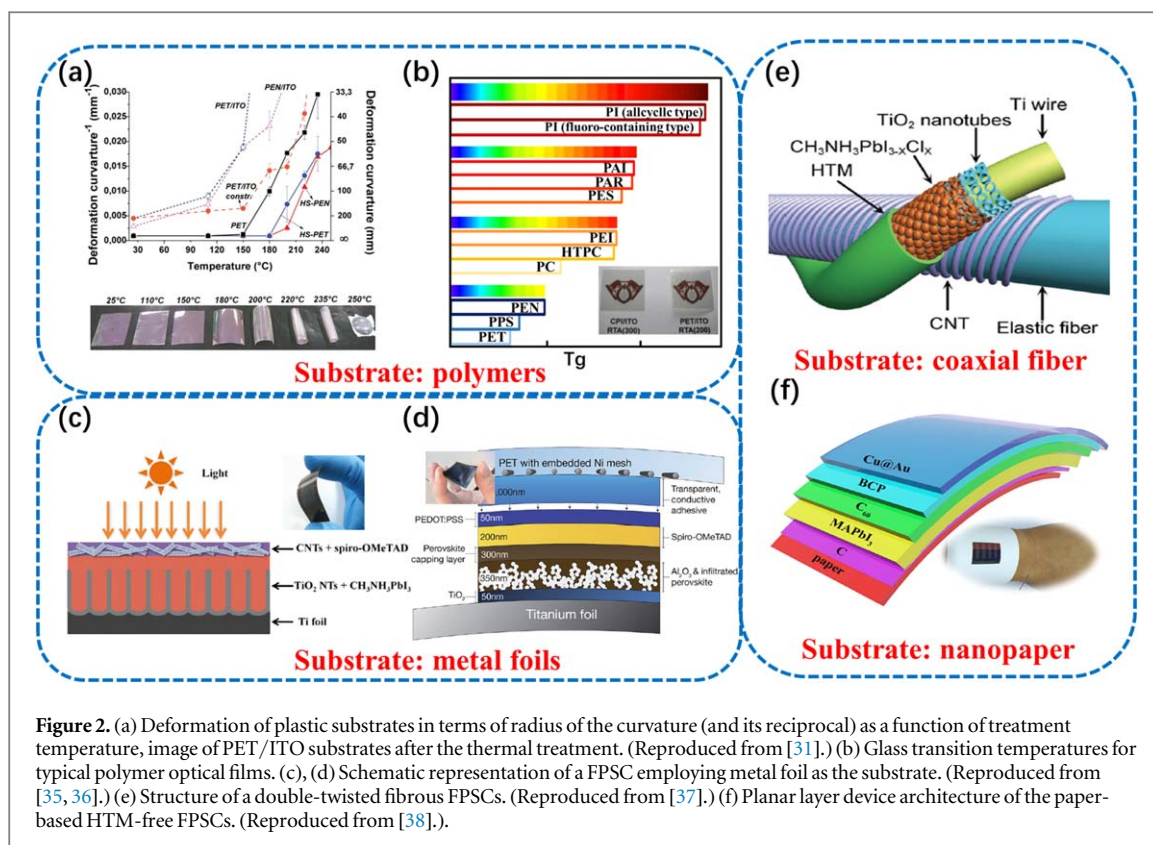


Figure 2. (a) Deformation of plastic substrates in terms of radius of the curvature (and its reciprocal) as a function of treatment temperature, image of PET/ITO substrates after the thermal treatment. (Reproduced from [31].) (b) Glass transition temperatures for typical polymer optical films. (c), (d) Schematic representation of a FPSC employing metal foil as the substrate. (Reproduced from [35, 36].) (e) Structure of a double-twisted fibrous FPSCs. (Reproduced from [37].) (f) Planar layer device architecture of the paper-based HTM-free FPSCs. (Reproduced from [38].)

metal substrates, these FPSCs require a top transparent conducting electrode (TCE) to guarantee the light absorption of the perovskite layer. Enlightened from the metal foil-based dye-sensitized solar cells, the titanium and copper foil can be a feasible alternative to polymer substrates [39]. Troughton *et al* prepared the titanium (Ti)-foil-based FPSCs via depositing a poly (3,4-ethylenedioxythiophene):poly(styrenesulfonate) (PEDOT:PSS)-covered nickel mesh upon the HTL as a transparent electrode (figure 2(c)); the PCE of this device is 10.3%, and it shows an excellent bending stability [35]. Wang and co-workers firstly proposed Ti metal foil substrate-based FPSCs and the device yielded a PCE of 8.31% (figure 2(d)) [36]. In another aspect, Lee and co-workers deposited ITO on the ultra-thin Ag top electrode and this method increased the PCE of FPSCs. The Ag/ITO offered outstanding excellent conductivity and transmittance. The efficiency of Ti metal substrate-based FPSCs significantly enhanced achieving a maximum PCE of 11.01% [40, 41]. Heo and co-workers fabricated FPSCs based on a flexible Ti substrate, the device achieved a PCE of 15.0% by changing the quantity of graphene layers upon the PDMS TE and the anodization time of the Ti metal substrate [42]. Apart from using a Ti substrate, copper (Cu) foil substrates are also a candidate. Recently, Nejang and co-workers used Cu foil as a substitute to replace Ti foil for FPSCs. They fabricated the devices with a structure Cu metal substrate/CuI/MAPbI₃/ZnO/AgNWs and the device achieved a PCE of 12.8% [43]. Based on previous research, the above substrates could not meet the

requirement of stretchable and foldable properties. Therefore, Qiu and co-workers fabricated a new type of FPSC upon the coaxial fibers. The multiwalled carbon nanotube electrode was continuously intertwined upon the fiber electrode. The fiber-shaped FPSCs achieved a PCE of 3.3% and this new type of FPSC remained stable under bending [44]. Li and co-workers replaced the metal-wire electrode with flexible CNT fibers, which created FPSCs with double twisting properties [45]. The flexible device yielded a maximum PCE of 3.03%. Meanwhile, the FPSC shows long-term environmental stability and outstanding bending resistance even in a bending cycle of more than 1000 times. Later, Deng and co-workers modified the conventional metal substrate and used the spring-like Ti wires and nano-structured fibers as electrodes. The corresponding structure is shown in figure 2(e). The FPSCs prepared based on the fiber state show superior flexibility and wearable ability than planar structure [37].

Another strategy to break the temperature restricted condition is to use an ultra-thin flexible glass. Flexible glass substrates with extra-thin thickness retain many of the benefits of rigid glass, for example, high temperature tolerance, remarkable moisture and oxygen barrier properties, and so on. These features are sufficient for flexible substrate requirements in FPSCs. Compared with the substrate materials listed above, the high cost and brittleness restrict the ultra-thin flexible glass widespread use and promotion. Nevertheless, the expensiveness and brittleness of ultra-thin glass will be a big problem compared to other flexible

Table 1. Summary of different substrates and the representative PCEs of FPSCs.

Substrates	CTE [ppm/°C]	Structure of FPSCs	PCE [%]	References
PET	15–33	PET/ITO/PTAA/FAPbI _{3-x} Br _x + MAPbI _{3-y} Br _y /fullerene/BCP/Cu	18.10	[51]
PDMS	10 ⁻⁴	PDMS/APTES/TFSA-doped graphene/PEDOT:PSS/FAPbI _{3-x} Br _x /PCBM/Al	18.00	[52]
PEN	20	PEN/Graphene/MoO ₃ /PEDOT:PSS/MAPbI ₃ /C60/BCP/LiF/Al	16.80	[27]
PEN	20	PEN/ITO/UV-Nb:TiO ₂ /MAPbI ₃ /spiro-OMeTAD/Au	16.01	[53]
PET	15–23	PET/ITO/TiO ₂ /MAPbI _{3-x} Br _x /PTAA/Au	15.88	[54]
PEN	20	PEN/ITO/ZnO/MAPbI ₃ /PTAA/Au	15.40	[55]
PET	15–23	PET/ITO/PEDOT:PSS/MAPbI ₃ /PNDI-2T + PCBM/LiF/Al	15.40	[56]
PEN	15–23	PEN/ITO/Zn ₂ SnO ₄ /MAPbI ₃ /PTAA/Au	15.30	[25]
CPI	8–20	Colorless PI/ITO/ZnO/MAPbI ₃ /PTAA/Au	15.20	[34]
PET	15–23	PET/ITO/am-TiO ₂ /MAPbI _{3-x} Cl _x /spiro-OMeTAD/Au	15.07	[57]
PET	15–23	PET/ITO/NiO _x /MAPbI ₃ /C60/Bis-C60/Ag	14.53	[58]
PET	15–23	PET/ITO/TiO ₂ (e-beam)/MAPbI _{3-x} Cl _x /PTAA/Au	13.50	[59]
Ti	—	Ti/anodized TiO ₂ /MAPbI ₃ /PTAA/graphene/PDMS	15.00	[42]
Ti	—	Ti/TiO ₂ /TiO ₂ NWs arrays/MAPbI ₃ /PEDOT/ITO/PEN	13.07	[60]
Cu	—	Cu/CuI/MAPbI ₃ /ZnO/Ag	12.80	[43]
Ti	—	Ti/TiO ₂ BL/TiO ₂ +MAPbI ₃ /Spiro/Ag+ITO	11.01	[41]
Ti	—	Ti/TiO ₂ /Al ₂ O ₃ /MAPbI _{3-x} Cl _x /spiro-OMeTAD/PEDOT:PSS/transparent	10.30	[35]
Willow glass	4	MgF ₂ /Willow glass/ITO/SnO ₂ /FAMACs/Spiro/MoO _x /Al	18.10	[47]
Cellulose paper	1	paper/Au/SnO ₂ /meso-TiO ₂ /CH ₃ NH ₃ PbI ₃ /Spiro-OMeTAD/MoO _x /Au/MoO _x	2.70	[61]

substrates. Tavakoli and co-workers used ultra-thin flexible glass as the substrate for the manufacture of PSC with a PCE of 12.06%. Subsequently, based on this method, a layer of nano-cone array anti-reflection film was integrated on the glass substrate, and the PCE of this device was improved to 13.14%, showing excellent optical transmittance and device performance [46]. More importantly, this improved method created a hydrophobic surface on the glass, enhanced the performance of gas barrier properties for oxygen and moisture, and the device exhibited excellent stability. Later studies have borrowed this strategy. Dou and co-workers fabricated an 18.1% efficiency of FPSCs by employing MgF₂ as an anti-reflection stratum and substituting ITO with indium zinc oxide (IZO) on ultra-thin flexible glass [47].

In addition, not only conventional materials are used: muscovite mica and nanostructures can also be used as a substrate in flexible perovskites. Fan and co-workers developed the nanostructured substrates by a simple method, the FPSCs' PCE reached up to 11.29%, which was fabricated based on i-cone substrates. The inverted nanocone structure represented a highly promising substrate owing to the beneficial light trapping effect and was highly robust and durable [48]. Jung and co-workers prepared a transparent electrode that is formed of three alternating layers (TiO_x/Ag/TiO_x, DMDA) via sputtering deposition. The devices based on this nano structure yielded a PCE of 6.37% [38]. Cellulose paper has also been used as substrate in FPSCs. Because of its low cost, abundant source, flexibility, biocompatibility, and approachability in terms of roll-to-roll large-area [38]. Gao and

co-workers firstly fabricated FPSCs on the cellulose paper substrate and the device reached an efficiency of 9.05% (figure 2(f)), the FPSC kept 75% of the original efficiency after 1000 bending cycles [49]. Muscovite mica seems to satisfied all the demands of flexible transparent substrates: low-cost, high-light transmittance, high-temperature tolerance, resistance to oxygen and water impermeability and high dimensional stability. This type of substrate allows a thermal treatment to prepare FPSCs with a high efficiency of 9.67% [50].

The device structure and representative performance of FPSCs fabricated upon various substrates are summarized in table 1. From the table data, it is apparent that the choice of substrate is important for fabricating a high-performance device. Undoubtedly, under the efforts of scientists, more and more new materials will be used as flexible substrates.

3. Transparent electrodes

A transparent electrode is an indispensable part of an FPSC. In order to yield an outstanding performance of FPSCs, the electrode materials used in FPSCs should have the following characteristics: superior flexibility, high transmittance, low electrical resistance. Particularly, excellent electrical conductivity is required for ideal electrodes in FPSCs. At present, there are four types of materials that have been proven for transparent electrodes; TCOs, metal-based materials, carbon-based materials, and conducting polymers have been employed as the electrodes in FPSCs.

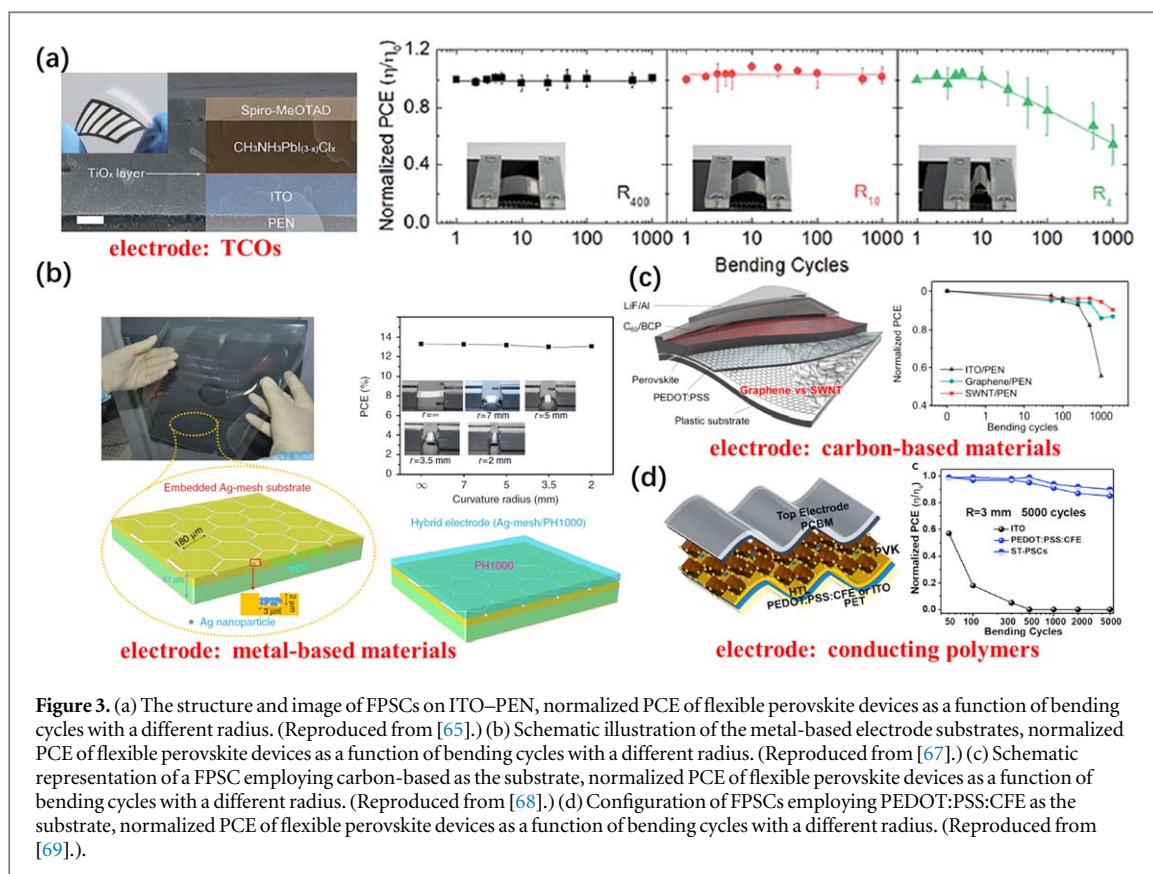


Figure 3. (a) The structure and image of FPSCs on ITO–PEN, normalized PCE of flexible perovskite devices as a function of bending cycles with a different radius. (Reproduced from [65].) (b) Schematic illustration of the metal-based electrode substrates, normalized PCE of flexible perovskite devices as a function of bending cycles with a different radius. (Reproduced from [67].) (c) Schematic representation of a FPSC employing carbon-based as the substrate, normalized PCE of flexible perovskite devices as a function of bending cycles with a different radius. (Reproduced from [68].) (d) Configuration of FPSCs employing PEDOT:PSS:CFE as the substrate, normalized PCE of flexible perovskite devices as a function of bending cycles with a different radius. (Reproduced from [69].).

Fluorine-doped tin oxide (FTO) and ITO are diffusely employed for FPSCs due to their unique features, which include excellent conductivity, high transmittance and good compatibility with perovskite [62]. To date, most devices are fabricated on this type substrates and the highest PCE is achieved from FPSCs based on ITO/PET substrates [28, 57, 63, 64]. For the fabrication of ITO-based glass, ITO is dc-magnetron sputtered at glass substrates while the substrate is maintained at approximately 300 °C–400 °C, or sputtered on the cold substrate, followed by annealing at 200 °C. Such a heat treatment would result in a high degree of the crystalline or partially crystalline microstructure of ITO. Meanwhile, it is apparent that the brittle characteristic of ITO will be impaired during the repeated bending course, which would lead to substrate resistance increase, and cracks appearing in the active layer [65]. Zardetto *et al* explored the regression course of ITO/PET and ITO/PEN after bending from 16 mm to 2 mm. When the radius was reduced to less than 14 mm, the thin layer resistance of the film significantly increased, indicating that the film had been damaged [31]. Kim and co-workers tested the FPSCs' detailed variation fabricated on the PEN/ITO substrate under bending [66]. This consequence indicates that the devices cause a sharp decline in efficiency after 10 bending cycles, as shown in figure 3(a).

In order to solve this challenge, metal-based electrode materials have been developed. Metal nanostructures, which include metal meshes, metal nanowires and ultra-thin metal films, had been proved

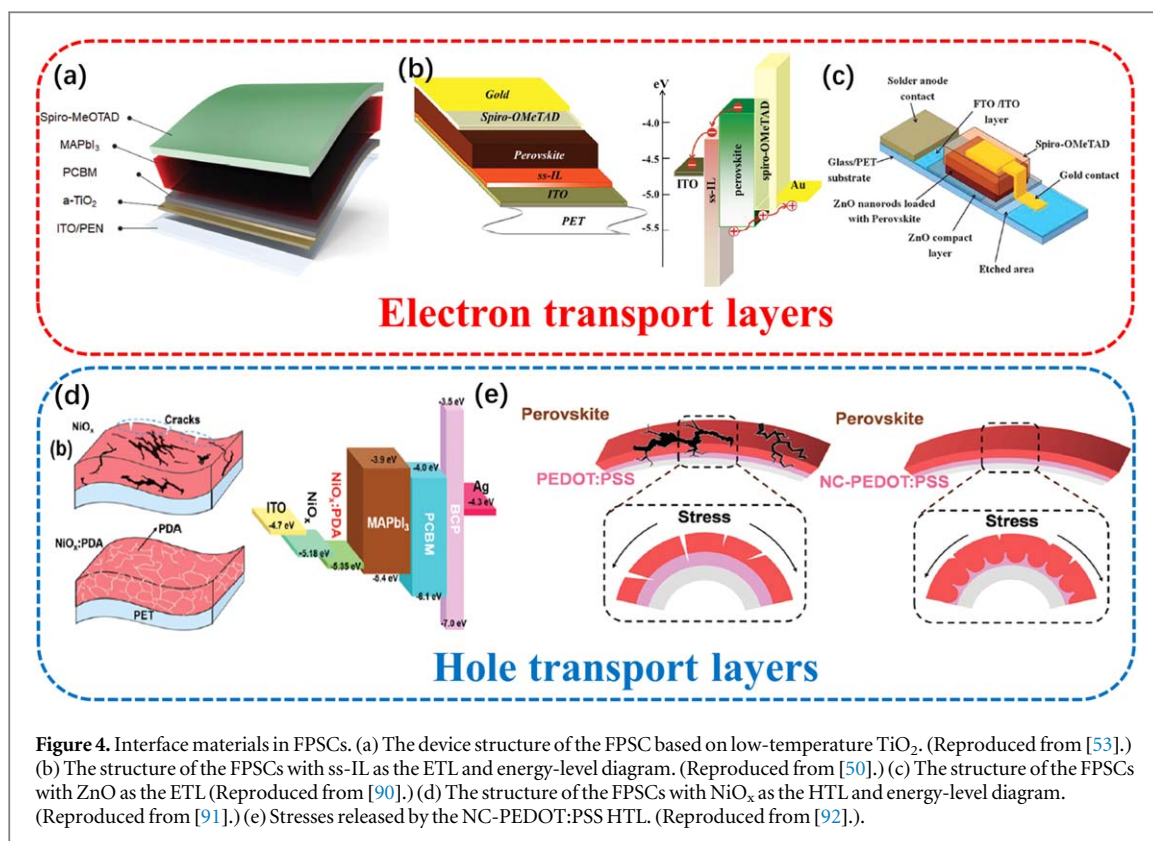
to be the substitute electrodes because of the high electrical conductivity, light transmittance and outstanding mechanical flexibility. Jun and co-workers used solution-treated Ag-NWs as electrodes and titanium as the substrate. The prepared FPSC has an efficiency of only 7.58% and the poor PCE is mainly attributed to the inferior conductivity of this electrode as compared to the ITO electrode [67]. Later, Li and co-workers fabricated high-performance FPSCs based on silver mesh/conducting polymer substrates, which show highly flexible and ultrathin characteristics, as shown in figure 3(b). The FPSC yielded a PCE of 14.0%. And there was almost no difference in performance compared to devices fabricated on rigid glass [70]. The FPSCs prepared by this method kept 98.1% of the primal PCE even tested under the ultimate bending radius (2 mm). The device has almost no degeneration and exhibited excellent bending resistance. Sears and co-workers fabricated the AgNW/PEDOT:PSS transparent electrode via a roll-to-roll slot-die technology. The electrode showed excellent light transmittance and electrical conductivity. The PCE of the FPSCs achieved 11% [71]. So as to enhanced the performance of AgNWs, Lee and co-workers covered the protective layer of amorphous aluminum doped zinc oxide (a-AZO) on the AgNW grid, the device achieved a PCE of 11.23% and 13.93% prepared on flexible and rigid substrates, respectively. The FPSCs with the a-AZO/AgNW/AZO composite electrode maintained 94% of the original efficiency under 400 bending iterations with a bending radius of

12.5 mm [72]. The main problem faced by metal-based electrode materials in FPSC is that halide ions in perovskite materials are proven to adverse chemical reactions at the interface with metals in transparent electrodes, which would significantly reduce the stability of PSC devices [39]. To avoid these shortcomings, Kaltenbrunner and co-workers introduced a chromium oxide-chromium interface layer into the FPSC, which could efficiently prevent from the diffusion between metal top contacts and the active layer. The pinhole-free perovskite films could deposit at low temperature on random substrates, including thin plastic foils, because of the employ of a transparent polymer electrode as the bottom layer, which was disposed with dimethylsulphoxide [73].

Metal electrodes were used in FPSCs usually need to be prepared under a high vacuum condition, which is not appropriate for large area manufacturing. At the same time, the expensive gold and silver electrodes limit the further commercialization of FPSCs. Therefore carbon-based electrode materials become an alternative electrode material in flexible solar cells because of their low sheet resistance, high transmittance, excellent conductivity, outstanding coverage, and easy manufacture by solution-processed approaches [74]. Owing to the network of conjugated double bonds, the nano carbon materials show high electrical conductivity and could be identified as one of the most attractive candidates for FPSCs. Wang and co-workers used a transparent carbon nanotube (CNTs) electrode to fabricated flexible device based on titanium foil substrate, achieving a PCE of 8.31% [36]. Later, Luo and co-workers prepared an inverted structure device employed a SnO₂-coated carbon nanotube (SnO₂@CSCNT) film as the electrode in FPSC, a PCE of 10.5% can be achieved on flexible substrates [75]. Jeon and co-workers selected single-walled carbon nanotubes (SWNT) as the transparent electrode, which was treated with nitric acid by a transfer technique and achieved a 5.38% PCE [68]. The deviations of SWNT and graphene, had been compared as the bottom electrode in an inverted structure (figure 3(c)). Both of them are commonly adopted as transparent carbon electrode materials. Due to the better morphology and higher transparency of the graphene-based PSCs, the photovoltaic performance was superior to the SWNT-based PSCs [76]. Graphene is another ideal alternative carbon-based electrode material for FPSCs, because of their high transmittance, outstanding carrier mobility, excellent charge conductivity and prominent environmental stability [77, 78]. The flexible devices with a structure of PET/graphene/poly(3-hexylthiophene)/CH₃NH₃PbI₃/PC₇₁BM/Ag were fabricated on 20 μm-thick PET substrates via a low-temperature solution method, which showed the PCE of 11.5% and desirable bending stability. This work paves a way for fabricating FPSCs as the same as other flexible devices by using graphene transparent electrodes. In order to

further decrease the high sheet resistance of graphene, doping methods were used to strengthen the interaction force between the PET substrate and graphene layer by introducing chemical bonding. Liu *et al* firstly demonstrated the fabrication of ultrathin FPSCs based on the graphene transparent flexible devices. Compared with the flexible ITO-based devices, the device yielded a comparable PCE of 16.8% with no hysteresis and showed outstanding stability against bending deformation. More importantly, the graphene-based device kept >90% of its initial PCE after 1000 cycles and 85% even after 5000 bending cycles with a bending radius of 2 mm [27]. Heo and co-workers introduced an APTES (3-aminopropyl triethoxysilane) adhesion promoter between the PET flexible substrate and AuCl₃-doped single-layer graphene transparent electrode. After the treatment of this method, a strong adhesion could generate between the graphene and the metal surface. The device fabricated on the AuCl₃-GR/APTES/PET substrate showed outstanding bending stability, holding its initial efficiency over 90% after 100 bending cycles [79]. Afterwards, they further enhanced the PCE to 18.3% by employing bis(tri uoromethanesulfonyl)-amide (TFSA)-doped graphene as the electrode for a FPSC. The TFSA dopant could improve the J_{sc} of the FPSC unlike the MoO₃ and AuCl₃ p-type dopants, which would not display absorption in the visible light region. This device also showed excellent bending stabilities as it retained 85% of its initial PCE after 5000 bending cycles at a radius of curvature of 12 mm [80]. In general, the graphene-based devices were more impressionable to tension than the carbon nanotube-based cells, though the diversities was tiny. Generally speaking, despite better performance, the transfer progress for graphene has poorer reproducibility [81].

In addition, conducting polymers have been adopted for another ideal alternative electrode material because of their outstanding conductivity with treatment, high transmittance, and excellent film processability [82]. Poly(3,4- ethylenedioxythiophene):poly(styrene sulfonate) (PEDOT:PSS) has been covered on polymer substrates as an electrode in FPSCs, the devices exhibit good flexibility. Dianetti and co-workers fabricated an inverted structure device employing a PEDOT:PSS (PH1000) to take the place of an ITO electrode on the PET substrate. This device obtained a poor PCE of 4.9%. However, under the condition of 100 bending cycles at radii down to 3 mm testing, the device maintained its original PCE value, showing the high flexibility. This report firstly demonstrated the excellent mechanical stability of TCO-free substrate-based FPSCs [82]. Poorkazem and co-workers compared two different FPSCs with two different transparent electrodes, PEDOT:PSS and ITO on PET substrates. The PEDOT:PSS electrodes show mechanical stability than ITO under a cylinder of 4 mm bending test for 2000 cycles, while the ITO electrodes appeared to have very obvious cracks, resulting in an



extremely high sheet resistance and device performance degradation [83]. Wu and co-workers used PEDOT:PSS as the electrode to fabricate FPSCs. PEDOT:PSS was spin-coated on PET substrates, followed by a nitric acid annealing to obtain the n-PEDOT:PSS bottom electrode. This device yielded 10.3% PCE and kept >90% of this original value after 1000 cycles of bending at a small radius of 5 mm [69]. More recently, Hu and co-workers utilized a mechanically robust conducting polymer network PEDOT:PSS electrode for FPSCs. This electrode consists of an ionic additive-conductivity and flexibility enhancer (CFE). The PEDOT:PSS:CFE simultaneously meets high conductivity, improved transmittance, and outstanding mechanical endurance. The device achieved a PCE of 19.0% and exhibits strong mechanical stability (figure 3(d)) [84].

4. Interface layers for FPSCs

The interface layers play significant roles in high-efficiency FPSCs, which includes the ETLs and HTLs. The interlayer materials require appropriate capabilities, such as enough transparency during the visible light, excellent carrier mobility, and desirable energy level assignment with the perovskite layers. In addition, an important key is that they can be prepared by low-temperature processes for FPSCs [85]. Next, the ETLs and HTLs developed for FPSCs recently will be introduced.

TiO₂ is a fashionable electronic transport layer utilized in PSCs due to its suitable workfunction and wide bandgap [86, 87]. Nevertheless, a significant defect of TiO₂ restricts its applications in FPSCs; TiO₂ films are often prepared employing spin-coating or spray pyrolysis, which need a high-temperature (>450 °C) sintering to yield a comparatively compact film with high crystallinity [57]. It is apparent that the high-temperature technique not only complicates the fabrication processes but also cannot be compatible with the soft polymer substrates widely used for FPSCs. There are two approaches to fabricate TiO₂ ETL on a flexible plastic substrate. Firstly, low-temperature deposition employing vacuum-based deposition techniques such as the evaporator, magnetron sputtering, and atomic layer deposition (ALD). Secondly, UV treatment or low-temperature annealing treatment are essential for high-quality TiO₂ colloidal particles [53, 88]. To work out this conundrum, many low-temperature techniques were put forward to prepare TiO₂. Yang and co-workers compared some representative amorphous and anatase TiO₂ layers, which include charge transport properties, recombination mechanisms, and carrier lifetime. The results show that the fermi level of amorphous TiO₂ is slightly lower than the anatase TiO₂. This result in glorious electron-transport performance of an amorphous layer, yielding an efficiency of 15.07% [57]. Jung *et al* employed the plasma-enhanced atomic layer deposition (PEALD) technique to prepared an about 20 nm-thick TiO_x compact layer at 80 °C. The PCE of the FPSCs based on this low-temperature process is up to 12.2% [77]. The TiO₂

ETL fabricated by PEALD are improved by interface modification with PCBM, the device achieved a PCE of 17.7% (figure 4(a)) [53]. Moreover, Giacomo and co-workers combined TiO₂ ETL fabricated by PEALD and TiO₂ layer as the electrode, based on this electrode, the resultant device achieved a PCE of 13.5% [89]. The mesoscopic TiO₂ layer can be prepared by electron-beam evaporation technique [59]. Although this method maintained the initial properties of TiO₂ porous layers, the preparation process is too intricate to be commonly employed. A solution-processed ionic liquid (IL) of 1-benzyl-3-methylimidazolium chloride was introduced as an ETL at room temperature (figure 4(b)). Yang and co-workers reported that the IL promotes the decline of the electron trap-state density at the active absorber surface. Thus, the infamous hysteresis in the current-density voltage curves had been effectively eliminated. Meanwhile, the PCE of the FPSCs, which used ss-IL as the ETL, was further enhanced to as high as 16.09%. The high efficiency could attribute to the distinct photoelectric properties of the ss-IL ETL, which involved a wide band gap, outstanding electron mobility, anti-reflection property, and well-aligned energy level with perovskite [62].

On account of the poor stability and infamous hysteresis of TiO₂ materials [59], researchers found other sorts of metal oxides to replace TiO₂. The substitute materials could fabricate in low temperatures conditions. Based on this, ZnO has become an ideal succedaneum for the ETL in FPSCs. The reason why ZnO can become a candidate mainly attributes to the higher electron mobility and the ZnO nanoparticle layer can be deposited easily by spin-coating without a high-temperature heating or sintering process [90]. In the original report of FPSCs, Kumar and co-workers used ZnO as the ETL to fabricate a FPSC as shown in figure 4(c); a chemical bath deposition (CBD) method was employed to prepare ZnO films. Although the PCE was low, only 2.62%, this work provides a method for low-temperature interface layers [93]. Later, Liu and co-workers spin-coated a butanol/chloroform ZnO mixture onto the ITO substrate. This approach needs no calcination or sintering process. The PCE of the FPSCs upon the comparatively compact ZnO layer exceeded 10% [94]. Subsequently, Heo and co-workers employed the ZnO layers with a 150 °C post-treatment for FPSCs and further improved the PCE to 15.5% [55]. But beyond that, Fan and co-workers put further questions about the reaction mechanism between perovskite and ZnO NPs, a quasi core-shell structure of ZnO/rGO QDs was used as the ETL to settle this problem. A stable FPSC had been obtained based on this hybrid structure, yielding a PCE of 11.2% [95]. Wang and co-workers found the tin oxide (SnO₂) ETL processed by low-temperature PEALD, which provides the prospect for preparing lightweight and efficient FPSCs. The reforming in device performance is mainly attributed to the enhanced conductivity and electrical mobility of SnO₂

ETL enabled by water vapor treatment. Consequently, the best FPSC fabricated on a commercial substrate exhibit a PCE of 18.36% [65].

New ETL materials have been utilized to improve charge transport as well as to decrease the hysteresis phenomenon in FPSCs. Zn₂SnO₄ (ZSO) is a good example, exhibiting better optical transmittance than SnO₂ [25]. The efficiency of ZSO-based FPSCs has been enhanced by tailoring particle size and stacking structure and the device achieves a PCE of 16.5% [26]. Also, the corporation of PCBM with ZSO was proved to promote electron transport in FPSCs [96]. Nb-doped WO_x (W(Nb)O_x) was chosen as the ETL. The device's PCE improved and the hysteresis phenomenon decreased by controlling the thickness of W(Nb)O_x [97]. Large bandgap materials such as Nb₂O₅ and Al₂O₃ were used as ETLs. The electron transport from the perovskite layer to TCO was enabled by quantum tunneling effect [98, 99]. Nevertheless, the intrinsic high series resistance is still limiting to yield high efficiency. As an alternative, conductive organic materials, which including the modified C₆₀ [100], 6,6-phenyl-C₆₁-butyric acid methyl ester (PC₆₁BM) [101], and N,N-bis(3-(dimethylamino)propyl)-N',N'-dimethylpropane-1,3-diamine (CDIN) [102], and so on, have been utilized as ETLs.

As for inorganic hole-transport materials, NiO_x materials have attracted more and more attention due to the well-matched band structure with an active layer, outstanding optical transparency, and electron blocking capability [103]. Najafi and co-workers fabricated NiO_x HTL via low-temperature solution coating methods (i.e. <150 °C) [91]. The devices achieved a 16.6% PCE for FPSCs, which showed fairly excellent stability. Over 85% of the maximum stabilized output PCE was maintained after 1000 h aging for the MAPbI₃ perovskite-based devices. Also, NiO_x derivatives have been applied to enhance photovoltaic performance. The device achieved an efficiency of 17.16%, which employed Cu-doped NiO_x (Cu:NiO_x) as the HTL. The high performance could attribute to the improved charge injection and the improved surface morphology of the NiO_x derivatives [104]. Recently, Duan and co-workers introduced a bendable nickel oxide (NiO_x) interfacial layer in FPSCs for the first time, which is fabricated via polydopamine (PDA) modification. PDA cross-linked NiO_x could release mechanical stress to eliminate the intrinsic brittleness of inorganic crystals as shown in figure 4(d). This flexible device retained >90% of this original efficiency after 1000 bending cycles [105].

In organic materials, 2,2',7,7'-tetrakis(N,N-di-p-methoxyphenylamine)-9,9'-spirobifluorene (spiro-OMeTAD) have been widely employed as HTL materials due to the well-matched energy level with an active layer, and the films can be easily prepared by low-temperature processes (i.e. <150 °C) [106]. Even though the high PCE has been obtained for FPSCs

employing spiro-OMeTAD as HTLs, there are still two adverse disadvantages: expensive cost and modest hole mobility conductivity [106]. Consequently, other HTL materials have been reported to replace spiro-OMeTAD to enhance the device performance. Based on the achievements above, PEDOT:PSS has been considered as an ideal candidate for HTL materials [107]. You and co-workers prepared the FPSC with a very simple PET/ITO/PEDOT:PSS/perovskite/PCBM/Al structure, the device achieved a PCE of 9.2% [108]. The worse device performance and long-term stability are attributed to the high acidity of PEDOT:PSS, which threatened to corrode the ITO electrode [92, 109]. In terms of this issue, Hu and co-workers reported a nanocellular scaffold, which released mechanical stresses during flexural experiences (figure 4(e)). The crystalline quality of the perovskite films could be significantly improved. Particularly, the device with the nanocellular optics resonant cavity structure exhibited outstanding performance, which including the sufficient light harvesting, effective charge transportation, excellent mechanical stability. This method was used to fabricate in modules as a wearable solar-power source, a PCE of 12.32% was yielded for a flexible large-scale device [110]. On the other hand, the carrier transport is comparatively worse in the out-of-plane direction due to the laminar structure. To solve this problem, new organic HTL materials such as 1,4-bis(4-sulfonatobutoxy)benzene and thiophene moieties (PhNa-1T) [111], Poly(triaryl amine) (PTAA) [103, 112] and (N-(4-(9H-carbazol-9-yl)phenyl)-7-(4-(bis(4-methoxyphenyl)amino)phenyl)-N-(7-(4-(bis(4-methoxyphenyl)amino)phenyl)-9,9-dioctyl-9H-fluoren-2-yl)-9,9-dioctyl-9H-fluoren-2-amine (CzPAF-TPA)) [113] have been exploited.

A summary of different ETLs, HTLs and the representative PCEs of FPSCs is shown in table 2. Different structures have different demands for interface layers. For example, in the n-i-p FPSCs structure, the ETL is deposited on the transparent electrodes, while the perovskite layer is covered with an HTL above it. So the selection for interface layer materials and depositing methods will influence the effective in extracting charge; beyond that, the performance of FPSCs will be seriously affected.

5. Large-area techniques

So far, most PSCs only fabricated based on small-area substrate. However, more and more large-area modules have also been reported in recent years, which is indispensable for FPSCs in future roll-to-roll production. In the translation of small-area to large-area devices, the following demands should be satisfied: (i) stable perovskite ink and large area coating techniques, (ii) optimized cell and interconnect design, and (iii) patterned deposition or post-patterning processes [92]. Giacomo and co-workers fabricated the large

area modules of $12.5 \times 13.5 \text{ cm}^2$ by slot die coating. This method ought to control the drying circumstance and the annealing atmosphere to guarantee the morphology for large-area FPSCs. The modules achieved a remarkable PCE of over 10% [51]. Razza and co-workers fabricated a series of connected modules of 100 cm^2 active area by sequential step deposition process. The PbI_2 layer deposited employing blade and spin coating technology, then dipped into a methylammonium iodide solution. In order to obtain the highly compact layers, the consequent optimization of the blade coating process and the dipping time should be controlled strictly. A module PCE of 4.3% was achieved for a 100 cm^2 active area [118]. Wang and co-workers used a scalable printing process to make perovskite modules with effective areas of 31 cm^2 and 70 cm^2 , and PCE of 10.46% and 10.74% were obtained [119]. Seo and co-workers reported a promising method towards a highly efficient PSC using a low-temperature solution-process and standard organic photovoltaic architecture. In this method, a flat and thick $\text{CH}_3\text{NH}_3\text{PbI}_3$ film and a thin PCBM film are prepared by the solution process at low temperature. The modules efficiency of 8.7% were achieved for an overall active area of 60 cm^2 a PCE [120].

The larger area perovskite thin films always have pinholes during the fabricating progress, which is due to the complex fluid dynamics [92]. Hence, Deng and co-workers showed that the surfactants (for example, $l\text{-}\alpha$ -Phosphatidylcholine) dramatically altered the fluid drying dynamics and increased the adhesion of the perovskite ink to the underlying non-wetting charge transport layer. The module efficiencies were stabilized at 15.3% and 14.6% for the active areas of 33.0 cm^2 and 57.2 cm^2 , respectively, by fast blading perovskite films [121]. Hu and co-workers have translated the low-cost hole-conductor free PSCs to a relative large area (100 cm^2). These perovskite solar modules were prepared by screen-printing, and 10 independent sub-cells were connected. The modules show a 10.4% PCE [122]. Heo and co-workers fabricated the inverted ITO/PEDOT:PSS/ MAPbI_3 /PCBM/Au planar hybrid solar sub-module. The sub-module with an overall active area of 40 cm^2 was obtained, and it exhibited power conversion efficiency of 12.9%. While a larger area 10-cell serially connected module (an overall active area of 40 cm^2) shows an 15.5% PCE [123, 124]. Chen and co-workers reported a novel strategy for methyl ammonium lead halide perovskite films, which does not depend on the general solvent or vacuum technicals. The perovskite solar module achieved a certified PCE of 12.1% with an active area of 36.1 cm^2 [125]. Jung and co-workers fabricated DHA-based modules at a size of $5 \text{ cm} \times 5 \text{ cm}$ (an overall active area of 24.94 cm^2) and used two different methods for depositing the P3HT layer, which are spin-coating and bar-coating specifically.

Table 2. Summary of different ETLs, HTLs and the representative PCEs of FPSCs.

	Interface layer	Required temperature [°C]	Structure of FPSCs	Note	PCE [%]	References
ETL	Nb ₂ O ₅	—	PET/ITO/Nb ₂ O ₅ /MAPbI ₃ /Spiro-OMeTAD/Au	Dimethyl sulfide additive	18.40	[114]
	SnO ₂ /C60-SAM	100	PET/ITO/treated SnO ₂ /C60-SAM/MA _{1-x} FaxPbI ₃ /Spiro-OMeTAD/Au	Water treated SnO ₂	18.36	[65]
	ss-IL	70	PET/ITO/ss-IL/(FAPbI ₃) _{0.85} (MAPbBr ₃) _{0.15} /Spiro-OMeTAD/Au	Solid-state ionic liquid	16.09	[62]
	TiO ₂	—	PET/ITO/TiO ₂ /MAPb(I _{1-x} Br _x) ₃ /PTAA/Au	RF sputtered TiO ₂	15.88	[54]
	c-TiO ₂ /BK-TiO ₂	—	PEN/ITO/c-TiO ₂ /BK-TiO ₂ /MAPbI ₃ /Spiro-OMeTAD/Au	Electro-deposited TiO ₂	15.76	[100]
	ZnO	150	PEN/ITO/ZnO/MAPbI ₃ /PTAA/Au	High mobility ETL, ZnO	15.60	[55]
	W(Nb)O _x	120	PEN/ITO/W(Nb)O _x /MAPbI _{3-x} Cl _x /Spiro-OMeTAD/Ag	W(Nb)O _x modified by Nb ⁵⁺	15.60	[97]
	TiO ₂	500	PET/ITO/TiO ₂ /CH ₃ NH ₃ PbI _{3-x} Cl _x /Spiro-OMeTAD/Au		15.10	[57]
	ZnSnO ₄	100	PEN/ITO/ZnSnO ₄ /MAPbI ₃ /PTAA/Au	Spin-coated ZnSnO ₄ ETL	14.90	[25]
	TiO ₂	—	PET/ITO/TiO ₂ /MAPbI _{3-x} Cl _x /PTAA/Au	Electron beam evaporated TiO ₂	13.50	[59]
	ZnO	—	Flexible glass/ITO/ZnO/MAPbI ₃ /Spiro-OMeTAD/Au		13.14	[115]
	HTL	PTAA	100	PET/ITO/PTAA/FAPbI _{1-x} Br _x /PCBM/C60/BCP/Cu		18.10
PEDOT:PSS		110	PEN/ITO/PEDOT:PSS/MAPbI ₃ /C60/BCP/LiF/Al		17.30	[27]
NiO _x		—	PET/ITO/NiO _x /MAPbI ₃ /PCBM + BIS-C60/Ag	Surface nanostructured HTM nanoparticle-based ink	14.50	[58]
PEDOT:PSS		110	PET/ITO/PEDOT:PSS/MAPbI ₃ /PCBM + LiF/Ag	PEI-HI layered perovskite at PEDOT interface	13.80	[116]
NiO _x		130	PET/ITO/NiO _x /MAPbI ₃ /PCBM/Ag	Spin-coated NiO _x nanoparticle	13.43	[117]

The performance of the modules was not undulant, with high PCEs of 16.3% and 16.0%, respectively [126]. Hong and co-workers successfully prepared high-efficiency, large-area PSC modules employing a new electrochemical patterning technique. By preparing planar-type PSC modules through low-temperature annealing and an all-solution method, a dramatically high efficiency of 14.0% with an area of 9.06 cm^2 and a high geometric fill factor of 94.1% was demonstrated [127]. Moreover, a new precursor system of $\text{Pb}(\text{CH}_3\text{CO}_2)_2 \cdot 3\text{H}_2\text{O}$, PbCl_2 , and $\text{CH}_3\text{NH}_3\text{I}$, obtaining highly crystalline perovskite films via a one-step spin-coating method followed by 10 min thermal annealing was developed. The high quality of the perovskite film enabled a 4 cm^2 aperture area perovskite module with a PCE of 13.6% [128].

Nevertheless, a fabricated large-area module with flexible substrate is a very efficient way of mass production based on a roll-to-roll (R2R) process, compared with the glass-based rigid substrate. But this useful way is at an early stage, so lots of effort has been focused on fabricating uniform ETLs or perovskite layers on large-area flexible substrates. For example, the large area uniform tin oxide layer resulted in serious hysteresis when printing it on rough and soft plastic substrates. Bu and co-workers used a universal potassium interfacial passivation strategy to resolve the hysteresis. The large size ($5 \times 6 \text{ cm}^2$) flexible modules obtain an efficiency over 15% [129]. This passivation method has shown a potential for obtaining high-performance large-area FPSCs. Galagan and co-workers first proved the possibility for the R2R slot die coating of the ETLs and the perovskite layers over the large area on flexible substrates with a width of 30 cm [130]. This achievement is a first solid step toward the future mass production of FPSCs. Although the feasibility of exploiting such a production process over large areas is a crucial intention of recent research, other techniques for large-area FPSCs fabrication, such as solution-shearing and spray-coating methods, have been developed. Similarly, crystal nucleation and growth in large-area perovskite thin films should be well controlled [131]. Rather, the devices fabricate on glass-based rigid substrates still reveal preponderant performance to their flexible counterparts. For example, Li and co-workers prepared a large-area PSC device on a glass/FTO-substrate with an active area $>1 \text{ cm}^2$, which achieved a PCE of 19.6% [132]. This is a value yet to be yielded by large-area PSC devices. In the same way, although large-area FPSCs have not be widely promoted and developed currently due to the low output efficiency, the ongoing development of such production processes are the key objective for future research.

6. Conclusion and outlook

In recent years, scientists have overcome many difficulties and solved many problems during the FPSCs research process. Among them, the choice of materials in each layer is crucial for building high-performance flexible perovskite solar cells. These materials include electrode materials, substrate materials and transport layer materials. We take into account every factor on the judgment of materials selection in both normal and inverted architectures. The PEN is the best substrate because of its excellent flexibility and transmittance, low cost and roll-to-roll processability, etc. Conducting polymers have been adopted for ideal electrode material because of their outstanding conductivity with treatment, high transmittance, and excellent film processability. As ideal transport materials, some inorganic and organic interface layer materials, including NiO_x , SnO_2 , PCBM, P3HT, have attracted more and more attention due to their enormous advantages. Compared with spiro-OMeTAD, these materials are not only cheap, but also easy to obtain stable ink, which improves the feasibility of fabricating flexible perovskite in large areas. In photovoltaic history, the FPSCs have continued to evolve, offering remarkable chances for various application fields. The superior PCE of FPSCs have been over 19%. And as reported, there have been some modules whose PCE have been more than 10%. Some niche applications for FPSCs can be achieved, such as electronic textiles, attachments on clothes, portable chargers and so on. A supposed 100 mW power output of the FPSCs can be used as a complementary source for electronics, such as smart watches, mobile phones and Fitbits etc. In recent years, even though it has been improved and promoted in terms of flexible substrates, transparent electrodes, interface layers and large area fabrications, the commercialization of FPSCs still faces several enormous challenges.

It is important for new techniques to fabricate the large-area flexible solar cells. Currently there are significant limitations in achieving large areas through roll-to-roll printing processes. Traditional techniques, such as anti-solvent treatment and a vacuum-assisted approach, bring challenges for the roll-to-roll printing process. The research of air-assisted processes, multi-component solvent and infrared post-treatment may provide direction for the new printing process. In addition, in the large-area preparation process, the quality of the film needs to be guaranteed, which puts higher requirements on the printing process. The FPSCs can be applied to more fields if the technique problem has been solved.

Another problem ought to be considered is the FPSCs should have certain environment universality. The solar cells can only generate the electricity under illumination of daylight but does not generate any energy in night time. This means that we should focus on how to broaden the spectral absorption range of

perovskite and application scenarios. Based on this, we can overcome this problem via fabricating tandem solar cells, such as laminating different types of PSCs or different types of devices.

Further exploration of strategy to improve FPSCs performance will become increasingly important for future developments in the field. The mechanical properties are the core problems of FPSCs. Foldable device products demand a small bending radius of curvature, which is comparatively challenging in foldable products made of inorganic electrical components. Also, many FPSCs contain inorganic materials including TCO, ETLs, and HTLs that are not favorable for reliable flexibility. Based on this, the mechanical properties can be enhanced by replacing or modifying inorganic TCO and substrate materials. The perovskite films' mechanical properties should also be improved by some strategies, such as additive engineers. The perovskite precursor solution and additives acted as physical or chemical cross-linking to make the films exhibit better mechanical properties. What is more the capabilities of perovskite films in the field of stretchable and twistable are crucial. There are two main ways to improve the stretchable and twistable capabilities, one of which is three dimensional-structure designs. Another solution is reducing the elastic modulus of perovskite crystals via new material design and molecular synthesis. Although textile PSCs offered the feasibility for the process of exploring integrating with cloth and skin, it is necessary to reduce the weight of the substrate and sealing layer as much as possible. In view of this question, the ultra-thin transparent rubber and cellulose paper have attracted a lot of attention. Many scientists tend to attach patterned FPSCs on the other parts of the device.

In order to realize the large-scale commercial production of FPSCs, while vigorously developing the above-mentioned PSC key technologies, it is also necessary to develop a thin film packaging technology with ultra-high water-oxygen barrier properties suitable for FPSCs. In order to realize the better application of the metal nanostructure transparent electrode on the FPSCs, it is necessary to further develop a technology that can effectively prevent the diffusion reaction between the halogen and the metal electrode in the perovskite material without affecting the efficiency of the device. In addition, the development of an inorganic electron and hole transport layer materials with low production cost and high stability compatibility are vital to large-scale applications in the future.

To sum up, great development space and vast prospective in FPSCs exist, so it is very necessary to vigorously develop the commercial flexible perovskite photovoltaics. Future research ought to focus on the widespread design idea and niche application from both perspectives of optoelectronics and mechanics. Based on this, the devices should satisfy the minimum input powers of relevant electronics and power storage systems. Therefore, there is no doubt that the FPSCs

will have a bright prospect if the efficiency and stability were improved. It is believed that FPSCs will become one of the most promising competitors for commercial solar cells.

Acknowledgments

Y C thanks for support from the National Natural Science Foundation of China (NSFC) (51673091 and 51833004), the National Science Fund for Distinguished Young Scholars (51425304) and NSFC-Guangdong Joint Funding, China (No. U1801256). L T thanks for the support from the National Natural Science Foundation of China (NSFC) (51672121). We also thank for support from Natural Science Foundation of Jiangxi Province (20161BBH80044, 20161BCB24004 and 20161ACB20020).

ORCID iDs

Xiaotian Hu  <https://orcid.org/0000-0001-5483-8800>

Licheng Tan  <https://orcid.org/0000-0001-7208-7297>

Yiwang Chen  <https://orcid.org/0000-0003-4709-7623>

References

- [1] Liu X, Jia L, Fan G, Gou J, Liu S F and Yan B 2016 Au nanoparticle enhanced thin-film silicon solar cells *Sol. Energy Mater. Sol. Cells* **147** 225–34
- [2] Liu X, Zi W and Liu S 2015 P-layer bandgap engineering for high efficiency thin film silicon solar cells *Mater. Sci. Semicond. Process.* **39** 192–9
- [3] Banerjee A, Su T, Beglau D, Pietka G, Liu F S, Almutawalli S, Yang J and Guha S 2012 High-efficiency, multijunction nc-Si:H-based solar cells at high deposition rate *IEEE J. Photovoltaics* **2** 99–103
- [4] Ren X, Zi W, Ma Q, Xiao F, Gao F, Hu S, Zhou Y and Liu S 2015 Topology and texture controlled ZnO thin film electrodeposition for superior solar cell efficiency *Sol. Energy Mater. Sol. Cells* **134** 54–9
- [5] Banerjee A, Liu F S, Beglau D, Su T, Pietka G, Yang J and Guha S 2012 12.0% efficiency on large-area, encapsulated, multijunction nc-Si:H-based solar cells *IEEE J. Photovoltaics* **2** 104–8
- [6] Battaglia C, Cuevas A and De Wolf S 2016 High-efficiency crystalline silicon solar cells: Status and perspectives *Energy Environ. Sci.* **9** 1552–76
- [7] Major J D 2016 Grain boundaries in CdTe thin film solar cells: a review *Semicond. Sci. Technol.* **31** 093001
- [8] Basol B M and McCandless B 2014 Brief review of cadmium telluride-based photovoltaic technologies *J. Photonics Energy* **4** 040996
- [9] Ramanujam J and Singh U P 2017 Copper indium gallium selenide based solar cells - a review *Energy Environ. Sci.* **10** 1306–19
- [10] Li W, Tan J M R, Leow S W, Lie S, Magdassi S and Wong L H 2018 Recent progress in solution-processed copper-chalcogenide thin-film solar cells *Energy Technol.* **6** 46–59
- [11] Dang W, Ren X, Zi W, Jia L and Liu S F 2015 Composition controlled preparation of Cu-Zn-Sn precursor films for $\text{Cu}_2\text{ZnSnS}_4$ solar cells using pulsed electrodeposition *J. Alloys Compd.* **650** 1–7

- [12] Zhao W, Pan D and Liu S 2016 Kesterite $\text{Cu}_2\text{Zn}(\text{Sn},\text{Ge})(\text{S},\text{Se})_4$ thin film with controlled Ge-doping for photovoltaic application *Nanoscale* **8** 10160–5
- [13] Wang D, Zhao W, Zhang Y and Liu S (Frank) 2018 Path towards high-efficient kesterite solar cells *J. Energy Chem.* **27** 1040–53
- [14] Liang D, Kang Y, Huo Y, Chen Y, Cui Y and Harris J S 2013 High-efficiency nanostructured window GaAs solar cells *Nano Lett.* **13** 4850–6
- [15] Hagfeldt A, Boschloo G, Sun L, Kloo L and Pettersson H 2010 Dye-sensitized solar cells *Chem. Rev.* **110** 6595–663
- [16] Carey G H, Abdelhady A L, Ning Z, Thon S M, Bakr O M and Sargent E H 2015 Colloidal quantum dot solar cells *Chem. Rev.* **115** 12732–63
- [17] Lu L, Zheng T, Wu Q, Schneider A M, Zhao D and Yu L 2015 Recent advances in bulk heterojunction polymer solar cells *Chem. Rev.* **115** 12666–731
- [18] Saparov B and Mitzi D B 2016 Organic-inorganic perovskites: structural versatility for functional materials design *Chem. Rev.* **116** 4558–96
- [19] Kojima A, Teshima K, Shirai Y and Miyasaka T 2009 Organometal halide perovskites as visible-light sensitizers for photovoltaic cells *J. Am. Chem. Soc.* **131** 6050–1
- [20] National Renewable Energy Laboratory (NREL) <https://www.nrel.gov/pv/cell-efficiency.html> (accessed: August 2019).
- [21] Podolsky B et al 2012 *Chem. Rev.* **338** 643–8 (references and notes 1)
- [22] Heo J H, Lee D S, Shin D H and Im S H 2019 Recent advancements in and perspectives on flexible hybrid perovskite solar cells *J. Mater. Chem. A* **7** 888–900
- [23] Su D et al 2015 The development of a highly photostable and chemically stable zwitterionic near-infrared dye for imaging applications *Chem. Commun.* **51** 3989–92
- [24] Jung J W, Williams S T and Jen A K Y 2014 Low-temperature processed high-performance flexible perovskite solar cells via rationally optimized solvent washing treatments *RSC Adv.* **4** 62971–7
- [25] Shin S S, Yang W S, Noh J H, Suk J H, Jeon N J, Park J H, Kim J S, Seong W M and Seok S I 2015 High-performance flexible perovskite solar cells exploiting Zn_2SnO_4 prepared in solution below 100 °C *Nat. Commun.* **6** 1–8
- [26] Shin S S, Yang W S, Yeom E J, Lee S J, Jeon N J, Joo Y C, Park I J, Noh J H and Seok S I 2016 Tailoring of electron-collecting oxide nanoparticulate layer for flexible perovskite solar cells *J. Phys. Chem. Lett.* **7** 1845–51
- [27] Yoon J, Sung H, Lee G, Cho W, Ahn N, Jung H S and Choi M 2017 Superflexible, high-efficiency perovskite solar cells utilizing graphene electrodes: towards future foldable power sources *Energy Environ. Sci.* **10** 337–45
- [28] Bi C, Chen B, Wei H, DeLuca S and Huang J 2017 Efficient flexible solar cell based on composition-tailored hybrid perovskite *Adv. Mater.* **29** 1–6
- [29] Cao B, Yang L, Jiang S, Lin H, Wang N and Li X 2019 Flexible quintuple cation perovskite solar cells with high efficiency *J. Mater. Chem. A* **7** 4960–70
- [30] Maniarasu S, Korukonda T B and Manjunath V 2018 Recent advancement in metal cathode and hole-conductor-free perovskite solar cells for low-cost and high stability: a route towards commercialization *Renew. Sustain. Energy Rev.* **82** 845–57
- [31] Zardetto V, Brown T M, Reale A and Di Carlo A 2011 Substrates for flexible electronics: a practical investigation on the electrical, film flexibility, optical, temperature, and solvent resistance properties *J. Polym. Sci., Part B: Polym. Phys.* **49** 638–48
- [32] Jiang N H, Gang L J, He W Z and Yong Y S 2015 A review on colorless and optically transparent polyimide films: chemistry, process and engineering applications *J. Ind. Eng. Chem.* **28** 16–27
- [33] Kang S B, Kim H J, Noh Y J, Na S I and Kim H K 2015 Face-to-face transferred multicrystalline ITO films on colorless polyimide substrates for flexible organic solar cells *Nano Energy* **11** 179–88
- [34] Park J I, Heo J H, Park S H, Hong K I, Jeong H G, Im S H and Kim H K 2017 Highly flexible InSnO electrodes on thin colourless polyimide substrate for high-performance flexible $\text{CH}_3\text{NH}_3\text{PbI}_3$ perovskite solar cells *J. Power Sources* **341** 340–7
- [35] Troughton J, Bryant D, Wojciechowski K, Carnie M J, Snaith H, Worsley D A and Watson T M 2015 Highly efficient, flexible, indium-free perovskite solar cells employing metallic substrates *J. Mater. Chem. A* **3** 9141–5
- [36] Wang X, Li Z, Xu W, Kulkarni S A, Batabyal S K, Zhang S, Cao A and Wong L H 2015 TiO_2 nanotube arrays based flexible perovskite solar cells with transparent carbon nanotube electrode *Nano Energy* **11** 728–35
- [37] Deng J, Qiu L, Lu X, Yang Z, Guan G, Zhang Z and Peng H 2015 Elastic perovskite solar cells *J. Mater. Chem. A* **3** 21070–6
- [38] Jung M H, Park N M and Lee S Y 2016 Color tunable nanopaper solar cells using hybrid $\text{CH}_3\text{NH}_3\text{PbI}_{3-x}\text{Br}_x$ perovskite *Sol. Energy* **139** 458–66
- [39] Wu Z, Li P, Zhang Y and Zheng Z 2018 Flexible and stretchable perovskite solar cells: device design and development methods *Small Methods* **2** 1800031
- [40] Lee M, Jo Y, Kim D S and Jun Y 2015 Flexible organo-metal halide perovskite solar cells on a Ti metal substrate *J. Mater. Chem. A* **3** 4129–33
- [41] Lee M, Jo Y, Kim D S, Jeong H Y and Jun Y 2015 Efficient, durable and flexible perovskite photovoltaic devices with Ag-embedded ITO as the top electrode on a metal substrate *J. Mater. Chem. A* **3** 14592–7
- [42] Heo J H, Shin D H, Lee M L, Kang M G and Im S H 2018 Efficient organic-inorganic hybrid flexible perovskite solar cells prepared by lamination of Polytriarylamine/ $\text{CH}_3\text{NH}_3\text{PbI}_3$ /Anodized Ti metal substrate and graphene/PDMS transparent electrode substrate *ACS Appl. Mater. Interfaces* **10** 31413–21
- [43] Abdollahi Nejad B, Nazari P, Gharibzadeh S, Ahmadi V and Moshaii A 2017 All-inorganic large-area low-cost and durable flexible perovskite solar cells using copper foil as a substrate *Chem. Commun.* **53** 747–50
- [44] Qiu L, Deng J, Lu X, Yang Z and Peng H 2014 Integrating perovskite solar cells into a flexible fiber *Angew. Chemie Int. Ed.* **53** 10425–8
- [45] Li R, Xiang X, Tong X, Zou J and Li Q 2015 Wearable double-twisted fibrous perovskite solar cell *Adv. Mater.* **27** 3831–5
- [46] Tavakoli M M, Tsui K H, Zhang Q, He J, Yao Y, Li D and Fan Z 2015 Highly efficient flexible perovskite solar cells with antireflection and self-cleaning nanostructures *ACS Nano* **9** 10287–95
- [47] Dou B et al 2017 High-performance flexible perovskite solar cells on ultrathin glass: implications of the TCO *J. Phys. Chem. Lett.* **8** 4960–6
- [48] Tavakoli M M, Lin Q, Leung S F, Lui G C, Lu H, Li L, Xiang B and Fan Z 2016 Efficient, flexible and mechanically robust perovskite solar cells on inverted nanocone plastic substrates *Nanoscale* **8** 4276–83
- [49] Gao C, Yuan S, Cui K, Qiu Z, Ge S, Cao B and Yu J 2018 Flexible and biocompatibility power source for electronics: a cellulose paper based hole-transport-materials-free perovskite solar cell (*Solar RRL* 11/2018) *Sol. RRL* **2** 1870224
- [50] Ke S, Chen C, Fu N, Zhou H, Ye M, Lin P, Yuan W, Zeng X, Chen L and Huang H 2016 Transparent indium tin oxide electrodes on muscovite mica for high-temperature-processed flexible optoelectronic devices *ACS Appl. Mater. Interfaces* **8** 28406–11
- [51] Di Giacomo F et al 2018 Up-scalable sheet-to-sheet production of high efficiency perovskite module and solar cells on 6-in. substrate using slot die coating *Sol. Energy Mater. Sol. Cells* **181** 53–9
- [52] Heo J H, Shin D H, Song D H, Kim D H, Lee S J and Im S H 2018 Super-flexible bis(trifluoromethanesulfonyl)-amide doped graphene transparent conductive electrodes for photo-stable perovskite solar cells *J. Mater. Chem. A* **6** 8251–8

- [53] Jeong I, Jung H, Park M, Park J S, Son H J, Joo J, Lee J and Ko M J 2016 A tailored TiO₂ electron selective layer for high-performance flexible perovskite solar cells via low temperature UV process *Nano Energy* **28** 380–9
- [54] Mali S S, Hong C K, Inamdar A I, Im H and Shim S E 2017 Efficient planar n-i-p type heterojunction flexible perovskite solar cells with sputtered TiO₂ electron transporting layers *Nanoscale* **9** 3095–104
- [55] Heo J H, Lee M H, Han H J, Patil B R, Yu J S and Im S H 2016 Highly efficient low temperature solution processable planar type CH₃NH₃PbI₃ perovskite flexible solar cells *J. Mater. Chem. A* **4** 1572–8
- [56] Heo J H, Jahandar M, Moon S J, Song C E and Im S H 2017 Inverted CH₃NH₃PbI₃ perovskite hybrid solar cells with improved flexibility by introducing a polymeric electron conductor *J. Mater. Chem. C* **5** 2883–91
- [57] Yang D, Yang R, Zhang J, Yang Z, Liu S and Li C 2015 High efficiency flexible perovskite solar cells using superior low temperature TiO₂ *Energy Environ. Sci.* **8** 3208–14
- [58] Zhang H, Cheng J, Lin F, He H, Mao J, Wong K S, Jen A K Y and Choy W C H 2016 Pinhole-free and surface-nanostructured niox film by room-Temperature solution process for high-performance flexible perovskite solar cells with good stability and reproducibility *ACS Nano* **10** 1503–11
- [59] Qiu W et al 2015 An electron beam evaporated TiO₂ layer for high efficiency planar perovskite solar cells on flexible polyethylene terephthalate substrates *J. Mater. Chem. A* **3** 22824–9
- [60] Xiao Y, Han G, Zhou H and Wu J 2016 An efficient titanium foil based perovskite solar cell: using a titanium dioxide nanowire array anode and transparent poly(3,4-ethylenedioxythiophene) electrode *RSC Adv.* **6** 2778–84
- [61] Castro-Hermosa S, Dagar J, Marsella A and Brown T M 2017 Perovskite solar cells on paper and the role of substrates and electrodes on performance *IEEE Electron Device Lett.* **38** 1278–81
- [62] Yang D, Yang R, Ren X, Zhu X, Yang Z, Li C and Liu S F 2016 Hysteresis-suppressed high-efficiency flexible perovskite solar cells using solid-state ionic-liquids for effective electron transport *Adv. Mater.* **28** 5206–13
- [63] Sakamoto K, Kuwae H, Kobayashi N, Nobori A, Shoji S and Mizuno J 2018 Highly flexible transparent electrodes based on mesh-patterned rigid indium tin oxide *Sci. Rep.* **8** 2825
- [64] Docampo P, Ball J M, Darwich M, Eperon G E and Snaith H J 2013 Efficient organometal trihalide perovskite planar-heterojunction solar cells on flexible polymer substrates *Nat. Commun.* **4** 2761
- [65] Wang C et al 2017 Water vapor treatment of low-temperature deposited SnO₂ electron selective layers for efficient flexible perovskite solar cells *ACS Energy Lett.* **2** 2118–24
- [66] Kim B J et al 2015 Highly efficient and bending durable perovskite solar cells: toward a wearable power source *Energy Environ. Sci.* **8** 916–21
- [67] Langley D, Giusti G, Mayousse C, Celle C, Bellet D and Simonato J P 2013 Flexible transparent conductive materials based on silver nanowire networks: a review *Nanotechnology* **24** 452001
- [68] Jeon I, Chiba T, Delacou C, Guo Y, Kaskela A, Reynaud O, Kauppinen E I, Maruyama S and Matsuo Y 2015 Single-walled carbon nanotube film as electrode in indium-free planar heterojunction perovskite solar cells: investigation of electron-blocking layers and dopants *Nano Lett.* **15** 6665–71
- [69] Zhang Y, Wu Z, Li P, Ono L K, Qi Y, Zhou J, Shen H, Surya C and Zheng Z 2018 Fully solution-processed TCO-free semitransparent perovskite solar cells for tandem and flexible applications *Adv. Energy Mater.* **8** 1701569
- [70] Li Y, Meng L, Yang Y, Xu G, Hong Z, Chen Q, You J, Li G, Yang Y and Li Y 2016 High-efficiency robust perovskite solar cells on ultrathin flexible substrates *Nat. Commun.* **7** 10214
- [71] Sears K K, Fievez M, Gao M, Weerasinghe H C, Easton C D and Vak D 2017 ITO-free flexible perovskite solar cells based on Roll-to-Roll, slot-die coated silver nanowire electrodes *Sol. RRL* **1** 1700059
- [72] Lee E, Ahn J, Kwon H C, Ma S, Kim K, Yun S and Moon J 2018 All-solution-processed silver nanowire window electrode-based flexible perovskite solar cells enabled with amorphous metal oxide protection *Adv. Energy Mater.* **8** 1702182
- [73] Kaltenbrunner M et al 2015 Flexible high power-per-weight perovskite solar cells with chromium oxide-metal contacts for improved stability in air *Nat. Mater.* **14** 1032–9
- [74] Kim K S, Zhao Y, Jang H, Lee S Y, Kim J M, Kim K S, Ahn J H, Kim P, Choi J Y and Hong B H 2009 Large-scale pattern growth of graphene films for stretchable transparent electrodes *Nature* **457** 706–10
- [75] Luo Q et al 2017 Carbon nanotube based inverted flexible perovskite solar cells with all-inorganic charge contacts *Adv. Funct. Mater.* **27** 1703068
- [76] Jeon I, Yoon J, Ahn N, Atwa M, Delacou C, Anisimov A, Kauppinen E I, Choi M, Maruyama S and Matsuo Y 2017 Carbon nanotubes versus graphene as flexible transparent electrodes in inverted perovskite solar cells *J. Phys. Chem. Lett.* **8** 5395–401
- [77] Wang J T W et al 2014 Low-temperature processed electron collection layers of graphene/TiO₂ nanocomposites in thin film perovskite solar cells *Nano Lett.* **14** 724–30
- [78] Liu Z, You P, Xie C, Tang G and Yan F 2016 Ultrathin and flexible perovskite solar cells with graphene transparent electrodes *Nano Energy* **28** 151–7
- [79] Heo J H, Shin D H, Jang M H, Lee M L, Kang M G and Im S H 2017 Highly flexible, high-performance perovskite solar cells with adhesion promoted AuCl₃-doped graphene electrodes *J. Mater. Chem. A* **5** 21146–52
- [80] Heo J H, Shin D H, Song D H, Kim D H, Lee S J and Im S H 2018 Super-flexible bis(trifluoromethanesulfonyl)-amide doped graphene transparent conductive electrodes for photo-stable perovskite solar cells *J. Mater. Chem. A* **6** 8251–8
- [81] Bae S et al 2010 Roll-to-roll production of 30-inch graphene films for transparent electrodes *Nat. Nanotechnol.* **5** 574–8
- [82] Dianetti M, Di Giacomo F, Polino G, Ciceroni C, Liscio A, D'Epifanio A, Licoccia S, Brown T M, Di Carlo A and Brunetti F 2015 TCO-free flexible organo metal trihalide perovskite planar-heterojunction solar cells *Sol. Energy Mater. Sol. Cells* **140** 150–7
- [83] Poorkazem K, Liu D and Kelly T L 2015 Fatigue resistance of a flexible, efficient, and metal oxide-free perovskite solar cell *J. Mater. Chem. A* **3** 9241–8
- [84] Hu X et al 2019 A mechanically robust conducting polymer network electrode for efficient flexible perovskite solar cells *Joule* **3** 2205–18
- [85] Yang D, Yang R, Priya S and Liu S (Frank) 2019 Recent advances in flexible perovskite solar cells: fabrication and applications *Angew. Chemie - Int. Ed.* **58** 4466–83
- [86] Jung H S and Park N G 2015 Perovskite solar cells: from materials to devices *Small* **11** 10–25
- [87] Boix P P, Nonomura K, Mathews N and Mhaisalkar S G 2014 Current progress and future perspectives for organic/inorganic perovskite solar cells *Mater. Today* **17** 16–23
- [88] Dkhissi Y, Huang F, Rubanov S, Xiao M, Bach U, Spiccia L, Caruso R A and Cheng Y B 2015 Low temperature processing of flexible planar perovskite solar cells with efficiency over 10% *J. Power Sources* **278** 325–31
- [89] Di Giacomo F et al 2015 Flexible perovskite photovoltaic modules and solar cells based on atomic layer deposited compact layers and UV-irradiated TiO₂ scaffolds on plastic substrates *Adv. Energy Mater.* **5** 1401808
- [90] Roldán-Carmona C, Malinkiewicz O, Soriano A, Mínguez Espallargas G, García A, Reinecke P, Kroyer T, Dar M I, Nazeeruddin M K and Bolink H J 2014 Flexible high efficiency perovskite solar cells *Energy Environ. Sci.* **7** 994–7
- [91] Najafi M et al 2018 Highly efficient and stable flexible perovskite solar cells with metal oxides nanoparticle charge extraction layers *Small* **14** 1702775
- [92] Di Giacomo F, Fakhruddin A, Jose R and Brown T M 2016 Progress, challenges and perspectives in flexible perovskite solar cells *Energy Environ. Sci.* **9** 3007–35

- [93] Kumar M H, Yantara N, Dharani S, Graetzel M, Boix P P and Mathews N 2013 Flexible, low-temperature, solution processed ZnO-based perovskite solid state solar cells *Chem. Commun.* **49** 11089–91
- [94] Liu D and Kelly T L 2014 Perovskite solar cells with a planar heterojunction structure prepared using room-temperature solution processing techniques *Nat. Photonics* **8** 133–8
- [95] Tavakoli M M, Tavakoli R, Nourbakhsh Z, Waleed A, Virk U S and Fan Z 2016 High efficiency and stable perovskite solar cell using ZnO/rGO QDs as an electron transfer layer *Adv. Mater. Interfaces* **3** 1500790
- [96] Liu X, Chueh C C, Zhu Z, Jo S B, Sun Y and Jen A K Y 2016 Highly crystalline Zn_2SnO_4 nanoparticles as efficient electron-transporting layers toward stable inverted and flexible conventional perovskite solar cells *J. Mater. Chem. A* **4** 15294–301
- [97] Wang K, Shi Y, Gao L, Chi R, Shi K, Guo B, Zhao L and Ma T 2017 $W(Nb)O_x$ -based efficient flexible perovskite solar cells: from material optimization to working principle *Nano Energy* **31** 424–31
- [98] Feng J, Yang Z, Yang D, Ren X, Zhu X, Jin Z, Zi W, Wei Q and Liu S (Frank) 2017 E-beam evaporated Nb_2O_5 as an effective electron transport layer for large flexible perovskite solar cells *Nano Energy* **36** 1–8
- [99] Wei J, Li H, Zhao Y, Zhou W, Fu R, Pan H and Zhao Q 2016 Flexible perovskite solar cells based on the metal-insulator-semiconductor structure *Chem. Commun.* **52** 10791–4
- [100] Yoon H, Kang S M, Lee J K and Choi M 2016 Hysteresis-free low-temperature-processed planar perovskite solar cells with 19.1% efficiency *Energy Environ. Sci.* **9** 2262–6
- [101] Qin F et al 2016 Indium tin oxide (ITO)-free, top-illuminated, flexible perovskite solar cells *J. Mater. Chem. A* **4** 14017–24
- [102] Zhu Z, Xu J Q, Chueh C C, Liu H, Li Z, Li X, Chen H and Jen A K Y 2016 A low-temperature, solution-processable organic electron-transporting layer based on planar coronene for high-performance conventional perovskite solar cells *Adv. Mater.* **28** 10786–93
- [103] Qiu Z, Gong H, Zheng G, Yuan S, Zhang H, Zhu X, Zhou H and Cao B 2017 Enhanced physical properties of pulsed laser deposited NiO films via annealing and lithium doping for improving perovskite solar cell efficiency *J. Mater. Chem. C* **5** 7084–94
- [104] He Q, Yao K, Wang X, Xia X, Leng S and Li F 2017 Room-temperature and solution-processable Cu-doped nickel oxide nanoparticles for efficient hole-transport layers of flexible large-area perovskite solar cells *ACS Appl. Mater. Interfaces* **9** 41887–97
- [105] Duan X, Huang Z, Liu C, Yang J, Tan L and Chen Y 2019 A bendable nickel oxide interfacial layer via polydopamine crosslinking for flexible perovskite solar cells *Chem. Commun.* **55** 3666–9
- [106] Saliba M et al 2016 A molecularly engineered hole-transporting material for efficient perovskite solar cells *Nat. Energy* **1** 15017
- [107] Brown T M, Kim J S, Friend R H, Cacialli F, Daik R and Feast W J 1999 Built-in field electroabsorption spectroscopy of polymer light-emitting diodes incorporating a doped poly(3,4-ethylene dioxythiophene) hole injection layer *Appl. Phys. Lett.* **75** 1679–81
- [108] Yang Y, You J, Hong Z, Chen Q, Cai M, Bin S T, Chen C C, Lu S, Liu Y and Zhou H 2014 Low-temperature solution-processed perovskite solar cells with high efficiency and flexibility *ACS Nano* **8** 1674–80
- [109] Niu J, Yang D, Ren X, Yang Z, Liu Y, Zhu X, Zhao W and Liu S (Frank) 2017 Graphene-oxide doped PEDOT:PSS as a superior hole transport material for high-efficiency perovskite solar cell *Org. Electron. physics, Mater. Appl.* **48** 165–71
- [110] Hu X et al 2017 Wearable large-scale perovskite solar-power source via nanocellular scaffold *Adv. Mater.* **29** 1703236
- [111] Jo J W et al 2016 Improving performance and stability of flexible planar-heterojunction perovskite solar cells using polymeric hole-transport material *Adv. Funct. Mater.* **26** 4464–71
- [112] Kim J, Yun J S, Wen X, Soufiani A M, Lau C F J, Wilkinson B, Seidel J, Green M A, Huang S and Ho-Baillie A W Y 2016 Nucleation and growth control of $HC(NH_2)_2PbI_3$ for planar perovskite solar cell *J. Phys. Chem. C* **120** 11262–7
- [113] Reddy S S, Shin S, Aryal U K, Nishikubo R, Saeki A, Song M and Jin S H 2017 Highly efficient air-stable/hysteresis-free flexible inverted-type planar perovskite and organic solar cells employing a small molecular organic hole transporting material *Nano Energy* **41** 10–7
- [114] Feng J, Zhu X, Yang Z, Zhang X, Niu J, Wang Z, Zuo S, Priya S, Liu S (Frank) and Yang D 2018 Record efficiency stable flexible perovskite solar cell using effective additive assistant strategy *Adv. Mater.* **30** 1801418
- [115] Qiu Y, Leung S F, Zhang Q, Hua B, Lin Q, Wei Z, Tsui K H, Zhang Y, Yang S and Fan Z 2014 Efficient photoelectrochemical water splitting with ultrathin films of hematite on three-dimensional nanophotonic structures *Nano Lett.* **14** 2123–9
- [116] Yao K, Wang X, Xu Y X and Li F 2015 A general fabrication procedure for efficient and stable planar perovskite solar cells: morphological and interfacial control by *in situ*-generated layered perovskite *Nano Energy* **18** 165–75
- [117] Yin X, Chen P, Que M, Xing Y, Que W, Niu C and Shao J 2016 Highly efficient flexible perovskite solar cells using solution-derived NiOx hole contacts *ACS Nano* **10** 3630–6
- [118] Razza S et al 2015 Perovskite solar cells and large area modules (100 cm^2) based on an air flow-assisted PbI_2 blade coating deposition process *J. Power Sources* **277** 286–91
- [119] Priyadarshi A, Haur L J, Murray P, Fu D, Kulkarni S, Xing G, Sum T C, Mathews N and Mhaisalkar S G 2016 A large area (70 cm^2) monolithic perovskite solar module with a high efficiency and stability *Energy Environ. Sci.* **9** 3687–92
- [120] Seo J, Park S, Chan Kim Y, Jeon N J, Noh J H, Yoon S C and Seok S I 2014 Benefits of very thin PCBM and LiF layers for solution-processed p-i-n perovskite solar cells *Energy Environ. Sci.* **7** 2642–6
- [121] Deng Y, Zheng X, Bai Y, Wang Q, Zhao J and Huang J 2018 Surfactant-controlled ink drying enables high-speed deposition of perovskite films for efficient photovoltaic modules *Nat. Energy* **3** 560–6
- [122] Hu Y, Si S, Mei A, Rong Y, Liu H, Li X and Han H 2017 Stable large-area ($10 \times 10\text{ cm}^2$) printable mesoscopic perovskite module exceeding 10% efficiency *Sol. RRL* **1** 1600019
- [123] Heo J H, Lee M H, Jang M H and Im S H 2016 Highly efficient $CH_3NH_3PbI_{3-x}Cl_x$ mixed halide perovskite solar cells prepared by re-dissolution and crystal grain growth via spray coating *J. Mater. Chem. A* **4** 17636–42
- [124] Heo J H, Han H J, Kim D, Ahn T K and Im S H 2015 Hysteresis-less inverted $CH_3NH_3PbI_3$ planar perovskite hybrid solar cells with 18.1% power conversion efficiency *Energy Environ. Sci.* **8** 1602–8
- [125] Chen H et al 2017 A solvent- and vacuum-free route to large-area perovskite films for efficient solar modules *Nature* **550** 92–5
- [126] Jung E H, Jeon N J, Park E Y, Moon C S, Shin T J, Yang T Y, Noh J H and Seo J 2019 Efficient, stable and scalable perovskite solar cells using poly(3-hexylthiophene) *Nature* **567** 511–5
- [127] Hong S et al 2018 High-efficiency large-area perovskite photovoltaic modules achieved via electrochemically assembled metal-filamentary nanoelectrodes *Sci. Adv.* **4** eaat3604
- [128] Qiu W et al 2016 Pinhole-free perovskite films for efficient solar modules *Energy Environ. Sci.* **9** 484–9
- [129] Bu T, Li J, Zheng F, Chen W, Wen X, Ku Z, Peng Y, Zhong J, Cheng Y B and Huang F 2018 universal passivation strategy to slot-die printed SnO_2 for hysteresis-free efficient flexible perovskite solar module *Nat. Commun.* **9** 4609
- [130] Galagan Y, Di Giacomo F, Gorter H, Kirchner G, de Vries I, Andriessen R and Groen P 2018 Roll-to-Roll slot die coated

- perovskite for efficient flexible solar cells *Adv. Energy Mater.* **8** 1801935
- [131] Li J et al 2017 Solution coating of superior large-area flexible perovskite thin films with controlled crystal packing *Adv. Opt. Mater.* **5** 1700102
- [132] Li X, Bi D, Yi C, Décoppet J D, Luo J, Zakeeruddin S M, Hagfeldt A and Grätzel M 2016 A vacuum flash-assisted solution process for high-efficiency large-area perovskite solar cells *Science (80-.)* **353** 58–62
- [133] Kim B J, Kim M C, Lee D G, Lee G, Bang G J, Jeon J B, Choi M and Jung H S 2018 Interface design of hybrid electron extraction layer for relieving hysteresis and retarding charge recombination in perovskite solar cells *Adv. Mater. Interfaces* **5** 1800993